Electronic Supplementary Material (ESI) for ChemComm.

—Supplementary Information—

Degradable Vinyl Copolymers through Thiocarbonyl Addition–Ring-Opening (TARO) Polymerization

*Nathaniel M. Bingham, Peter J. Roth**

Department of Chemistry, University of Surrey, Guildford, Surrey, GU2 7XH, United Kingdom

Contents

1) Instrumentation and general remarks

NMR spectroscopic measurements were performed on 400 or 500 MHz Bruker instruments in 5 mm NMR tubes. Residual solvent signals of $CHCl_3$ (δ_H = 7.26 ppm, δ_C = 77.2 ppm), and CD_2HCN (δ_H = 1.94 ppm) were used as references.

Fourier transform infrared spectroscopy (FT-IR) was performed on an Agilent Cary 600 Series spectrometer under attenuated total reflection (ATR).

Size exclusion chromatography (SEC) was performed on a Viscotek GPCMax VE 2001 setup with three linear 7.5×300 mm PLgel mixed-D columns connected to a Viscotek VE3580 refractive index (RI) detector and a Malvern 270 dual detector (viscometer and light scattering). The instrument operated at 35 °C with tetrahydrofuran (THF) containing 250 ppm BHT as mobile phase at a flow rate of 1.0 mL×min^{-1}. The system was calibrated using a series of narrow molecular weight distribution PMMA standards with molecular weights ranging from 5 kg×mol^{-1} to 298 kg×mol^{-1}.

Electrospray (ESI) mass spectra were recorded with an Orbitrap Q-Exactive Plus (Thermo UK) at a resolving power of 280,000 at 200 m/z. Data was acquired in negative ion mode at a scan range of 100–500 m/z. Samples were prepared in methanol–water 9:1.

Chemical ionisation mass spectra were recorded on an Agilent technologies 6550 ifunnel Q-TOF LC-MS instrument. Data was acquired in positive ion mode and samples were prepared in acetonitrile.

The structural optimization of DOT was performed using the Gaussian09 (version 8.0) software package. The optimization method involved a ground state DFT calculation with B3LYP functional and 6-311G basis set.

Materials. All reagents were purchased from Sigma-Aldrich and used as received. 2,2'-Azobis(isobutyronitrile) (AIBN) was recrystallized from methanol and stored in a freezer.

2) Synthesis of lactones

2.1) 3-Ethylphthalide

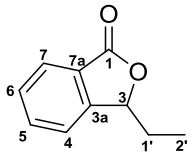

$C_{10}H_{10}O_2$

162.19 gmol^{-1}

Adapted from the work of Sheng *et al.,*[1] 2-carboxybenzaldehyde (500.4 mg, 3.33 mmol) was dissolved in anhydrous Et_2O (30 mL) and cooled to 0 °C. Ethylmagnesium bromide (2.3 mL, 6.99 mmol, 2.1 eq.) was then added dropwise over the course of 15 minutes. After 4 hours, the mixture was quenched with aq. HCl (0.2 M, 30 mL) and the organics were extracted with Et_2O (2 × 30 mL), combined, dried ($MgSO_4$) and concentrated *in vacuo*. The crude product was purified by column chromatography (EtOAc–pet. ether, 1:2) to afford a clear colourless oil (324.9 mg, 60%).

^{1}H NMR (400 MHz, $CDCl_3$) δ/ppm = 7.90 (d, *J* = 7.6 Hz, 1H, **7**), 7.68 (t, *J* = 7.3 Hz, 1H, **6**), 7.53 (t, *J* = 7.5 Hz, 1H, **5**), 7.45 (dd, *J* = 7.6, 0.7 Hz, 1H, **4**), 5.46 (dd, *J* = 6.8, 4.6 Hz, 1H, **3**), 2.20 – 2.06 (m, 1H, **1'**), 1.89 – 1.78 (m, 1H, **1'**), 1.00 (t, *J* = 7.4 Hz, 3H, **2'**).

^{13}C NMR (101 MHz, $CDCl_3$) δ/ppm = 170.68 (**1**), 149.75 (**3a**), 133.96 (**5**), 129.06 (**6**), 126.33 (**7a**), 125.65 (**7**), 121.76 (**4**), 82.31 (**3**), 27.65 (**1'**), 8.82 (**2'**).

2.2) Dibenzo[c,e]oxepan-5-one

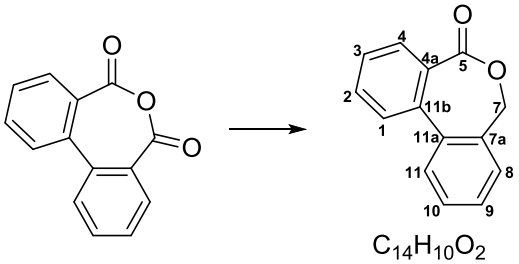

$C_{14}H_{10}O_2$
210.23 $gmol^{-1}$

In analogy to a procedure from Brandmeyer *et al.*,[2] diphenic anhydride (8.00 g, 35.7 mmol) was suspended in DMF (45 mL) and cooled to 0 °C before sodium borohydride (1.39 g, 36.7 mmol, 1.03 eq.) was added slowly. After 2 hours, the reaction mixture was poured into aq. HCl (6 M, 36 mL), which was then subsequently diluted with water (107 mL) and stirred overnight. The product precipitated overnight and was filtered before being taken up in dichloromethane (250 mL) and washed with water (5 × 200 mL). The organic layer was dried ($MgSO_4$), filtered, concentrated *in vacuo*, filtered through basic alumina with dichloromethane, and dried to afford a white powder (5.91 g, 79%).

^{1}H NMR (400 MHz, $CDCl_3$) δ/ppm = 8.00 (dd, *J* = 7.8, 0.9 Hz, 1H, **4**), 7.65 (m, 3H, **2**), 7.56–7.50 (m, 2H, **3**), 7.49–7.41 (m, 2H, **8**), 5.03 (d, *J* = 23.8 Hz, 2H, **7**).

^{13}C NMR (101 MHz, CDCl3) δ/ppm = 170.37 (**5**), 139.11, 137.40 (**4a**), 134.97, 132.70 (**2**) 132.07 (**4**), 130.81, 130.27, 128.82, 128.80, 128.71 (**8**), 128.69, 128.56 (**3**), 69.31 (**7**).

IR ν_{max}/cm^{-1} = 3070 (w, CH), 2950 (w, CH), 2902 (w, CH), 1700 (s, C=O), 1598 (m, C=C), 1560 (m, C=C).

Rf 0.61 (dichloromethane)

3) Synthesis of thionolactones

Generally, the lactone (1 eq) was dissolved in anhydrous toluene. Lawesson's Reagent (0.6 eq) was added and the mixture was refluxed overnight. Upon completion, the reaction mixture was filtered and concentrated *in vacuo*. Products were purified by column chromatography.

3.1) γ-Phenyl-γ-butyrothionolactone, **1**

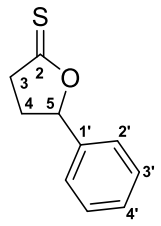

$C_{10}H_{10}OS$
178.25 $gmol^{-1}$

γ -Phenyl-γ-butyrolactone (3.01 g, 18.57 mmol) was dissolved in anhydrous toluene (300 mL) before an addition of Lawesson's Reagent (4.50 g, 11.13 mmol, 0.6 eq) and was refluxed for 22 hours. Upon completion, the reaction mixture was concentrated *in vacuo*. The crude product was purified by column chromatography (Hex–EtOAc, 9:1) and recrystallized from diethyl ether to afford colourless needles (932.0 mg, 28%).

^{1}H NMR (400 MHz, $CDCl_3$) δ/ppm = 7.45 – 7.33 (m, 5H, **2' – 4'**), 5.86 (dd, *J* = 8.5, 6.8 Hz, 1H, **5**), 3.28 (ddd, *J* = 18.8, 8.7, 4.2 Hz, 1H, **3**), 3.15 (ddd, *J* = 18.7, 9.5, 8.7 Hz, 1H, **3**), 2.70 (dddd, *J* = 12.9, 8.7, 6.7, 4.2 Hz, 1H, **4**), 2.29 (ddt, *J* = 12.8, 9.5, 8.6 Hz, 1H, **4**).
^{13}C NMR (101 MHz, $CDCl_3$) δ/ppm = 221.97 (**2**), 138.16 (**1'**), 129.02 (**4'**), 128.98 (**3'**), 125.91 (**2'**), 90.89 (**5**), 45.06 (**3**), 32.54 (**4**).
IR ν_{max}/cm^{-1} = 2981 (w, CH), 2956 (w, CH), 2904 (w, CH), 1493 (m, C=C), 1452 (m, C=C), 1136 (s, C=S).
Rf (dichloromethane) 0.85
MP 55.5–56.5 °C (from dichloromethane)
HR-MS (ESI) *m*/*z* calculation for $C_{10}H_{10}OS$ $[M-H]^-$ 177.0380, found 177.0371

3.2) 2-Benzofuran-1(3H)-thione, **2**

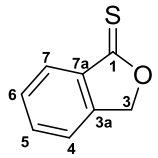

C_8H_6OS
150.20 $gmol^{-1}$

Phthalide (1.03 g, 7.71 mmol) was dissolved in anhydrous toluene (90 mL) before an addition of Lawesson's Reagent (1.81 g, 4.48 mmol, 0.6 eq) and was refluxed for 21 hours. Upon completion the reaction mixture was concentrated *in vacuo* and then taken up in Et_2O (90 mL) and cooled to −20 °C. A white solid was filtered away and the crude material was concentrated *in vacuo* before being purified by column chromatography (Hex–EtOAc, 9:1). The product was recrystallized from diethyl ether to afford yellow needles (722.8 mg, 62%).

^{1}H NMR (400 MHz, $CDCl_3$) δ/ppm = 8.07 (d, *J* = 7.8, 1.0 Hz, 1H, **7**), 7.69 (td, *J* = 7.5, 1.0 Hz, 1H, **5**), 7.58 – 7.48 (m, 2H, **4** & **6**), 5.58 (s, 2H, **3**).

^{13}C NMR (101 MHz, $CDCl_3$) δ/ppm = 211.13 (**1**), 144.82 (**3a**), 136.98 (**7a**), 133.94 (**5**), 129.39 (**6**), 127.05 (**7**), 121.47 (**4**), 77.82 (**3**).

IR ν_{max}/cm^{-1} 3024 (w, CH), 2954 (w, CH), 2926 (w, CH), 2877 (w, CH), 1450 (m, C=C), 1433 (m, C=C), 1134 (s, C=S).

Rf (dichloromethane) 0.85

MP 102–104 °C (from dichloromethane)

HR-MS (ESI) *m*/*z* calculation for C_8H_8OS $[M-H]^-$ 149.067, found 149.0056

3.3) 6-Nitro-2-benzofuran-1(3H)-thione, **3**

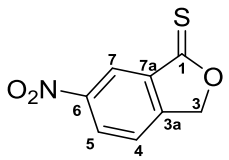

$C_8H_5NO_3S$
195.19 $gmol^{-1}$

6-Nitrophthalide (499.5 mg, 2.79 mmol) was dissolved in anhydrous toluene (50 mL) before an addition of Lawesson's Reagent (662.5 mg, 1.64 mmol, 0.6 eq) and was refluxed for 18 hours. Upon completion the reaction mixture was concentrated *in vacuo*. The crude product was purified by column chromatography (dichloromethane) to afford a yellow crystals (40.9 mg, 7.5%).

^{1}H NMR (400 MHz, $CDCl_3$) δ/ppm = 8.85 (d, *J* = 1.9 Hz, 1H, **7**), 8.56 (dd, *J* = 8.3, 2.1 Hz, 1H, **5**), 7.71 (dd, *J* = 8.3, 0.7 Hz, 1H, **4**), 5.69 (s, 2H, **3**).

^{13}C NMR (101 MHz, $CDCl_3$) δ/ppm = 207.45 (**1**), 149.80 (**3a**), 149.49 (**6**) 138.26 (**7a**), 128.30 (**5**), 123.08 (**4**), 122.32 (**7**), 77.51 (**3**).

IR ν_{max}/cm^{-1} = 3093 (w, CH), 3052 (w, CH), 3033 (w, CH), 2941 (w, CH), 2854 (w, CH), 1612 (m, C=C), 1599 (m, C=C), 1511 (s, NO_2), 1298 (s, NO_2) 1164 (m, C=S).

Rf (dichloromethane) 0.67

MP 158–159 °C (from dichloromethane)

HR-MS (ESI) *m*/*z* calculation for $C_8H_5NO_3S$ $[M-H]^-$ 193.9917, found 193.9911

3.4) 5-Cyano-2-benzofuran-1(3H)-thione, **4**

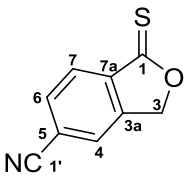

C_9H_5NOS
175.21 $gmol^{-1}$

5-Cyanophthalide (498.4 mg, 3.13 mmol) was dissolved in anhydrous toluene (50 mL) before an addition of Lawesson's Reagent (786.5 mg, 1.94 mmol, 0.6 eq) and was refluxed for 18 hours. Upon completion the reaction mixture was concentrated *in vacuo*. The crude product was purified by column chromatography (dichloromethane) to afford yellow crystals (92.2 mg, 17%).

^{1}H NMR (400 MHz, $CDCl_3$) δ/ppm = 8.13 (d, *J* = 8.0 Hz, 1H, **7**), 7.84 (s, 1H, **4**), 7.80 (d, 8.1 Hz, 1H, **6**), 5.64 (s, 2H, **3**).

^{13}C NMR (101 MHz, $CDCl_3$) δ/ppm = 207.95 (**1**), 144.76 (**3a**), 139.52 (**7a**), 133.12 (**6**), 127.66 (**7**), 126.04 (**4**), 117.76 (**1'**), 117.07 (**5**), 77.34 (**3**).

IR ν_{max}/cm^{-1} = 3081 (w, CH), 3028 (w, CH), 2924 (w, CH), 2850 (w, CH), 2227 (w, CN), 1448 (w, C=C), 1430 (w, C=C), 1132 (s, C=S).

Rf (dichloromethane) 0.59; **MP** 192–193 °C (from dichloromethane)

3.5) 3-Ethyl-2-benzofuran-1(3H)-thione, **5**

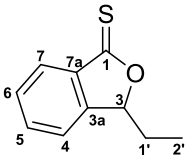

$C_{10}H_{10}OS$
178.25 $gmol^{-1}$

3-Ethylphthalide (324 mg, 2.00 mmol) was dissolved in anhydrous toluene (16 mL) before an addition of Lawesson's Reagent (519 mg, 4.48 mmol, 0.6 eq) and was refluxed for 26 hours. Upon completion the reaction mixture was filtered and concentrated *in vacuo* before being purified by column chromatography (Pet. ether–EtOAc, 3:1) to afford a dark yellow oil (306 mg, 86%).

^{1}H NMR (500 MHz, $CDCl_3$) δ/ppm = 8.03 (d, *J* = 7.8 Hz, 1H, **7**), 7.67 (t, *J* = 7.5 Hz, 1H, **5**), 7.51 (t, *J* = 7.6 Hz, 1H, **6**), 7.42 (d, *J* = 7.7, 1H, **4**), 5.71 (dd, *J* = 6.9, 4.6 Hz, 1H, **3**), 2.24 – 2.16 (m, 1H, **1'**), 1.97 – 1.88 (m, 1H, **1'**), 1.01 (t, *J* = 7.4 Hz, 3H, **2'**).

^{13}C NMR (101 MHz, $CDCl_3$) δ/ppm = 210.67 (**1**), 149.69 (**3a**), 137.14 (**7a**), 133.83 (**5**), 129.41 (**6**), 126.97 (**7**), 121.28 (**4**), 91.17 (**3**), 27.44 (**1'**), 8.93 (**2'**).

IR ν_{max}/cm^{-1} = 2970 (w, CH), 2933 (w, CH), 2877 (w, CH), 1610 (m, C=C), 1589 (m, C=C), 1163 (s, C=S).

Rf (EtOAc–Pet. Ether, 1:3) 0.54

3.6) Dibenzo[c,e]oxepan-5-thione, DOT, **6**

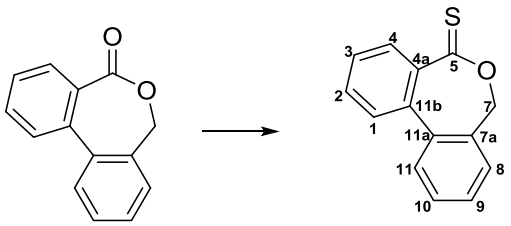

Lactone dibenzo[c,e]oxepan-5-one (4.69 g, 22.29 mmol) was dissolved in anhydrous toluene (350 mL) before an addition of Lawesson's Reagent (5.32 g, 11.13 mmol, 0.6 eq) and was refluxed for 22 hours. Upon completion the reaction mixture was concentrated *in vacuo* and purified by column chromatography (Hex–EtOAc, 4:1) to afford yellow crystals (2.04 g, 41%).

^{1}H NMR (400 MHz, $CDCl_3$) δ/ppm = 8.18 (d, *J* = 7.9 Hz, 1 H, **4**), 7.63 (d, *J* = 7.8 Hz, 1 H), 7.59 (t, *J* = 7.6 Hz, 1 H), 7.52 (m, 2 H), 7.46–7.40 (m, 3 H), 5.22, 5.14 (2 d, *J* = 11.5 Hz, 2 H, **7**).

^{13}C NMR (101 MHz, $CDCl_3$) δ/ppm = 216.1 (**5**), 139.1, 139.1, (**11a**, **11b**) 134.6, 134.5 (**4a**, **7a**), 134.0 (**4**), 132.1 (**3**), 130.4, 128.8, 128.6, 128.4 (**8**), 128.1, 73.8 (**7**).

IR ν_{max}/cm^{-1} = 3052 (w, CH), 2919 (w, CH), 2852 (w, CH), 1595 (m, C=C), 1556 (m, C=C), 1192 (m, C=S).

UV-Vis λ_{max}(MeCN) /nm = 207 (ε /$Lmol^{-1}cm^{-1}$ = 22,160), 238 (15,359), 279 (9,068), 315sh (5,866), 428 (409).

Rf 0.72 (EtOAc–Pet. Ether, 1:2)

Melting Point: 134–135 °C (from dichloromethane).

HR-MS (APCI) *m/z Calculated* mass for $C_{14}H_{10}SO + H^+$ = 227.0531,

found mass for $C_{14}H_{10}SO + H^+$ = 227.0539

Elemental Analysis Found: C, 74.1; H, 4.6. Calc. for $C_{14}H_{10}OS$: C, 74.3; H, 4.5%

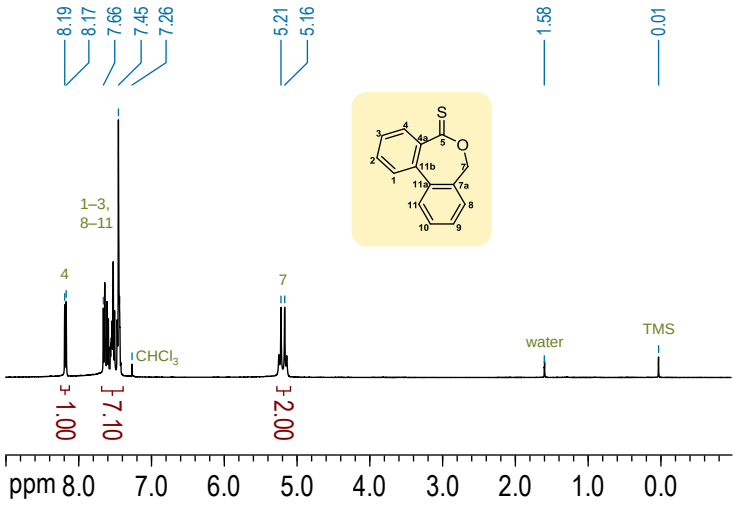

Figure S1. ^{1}H NMR spectrum (400 MHz, $CDCl_3$) of dibenzo[c,e]oxepan-5-thione.

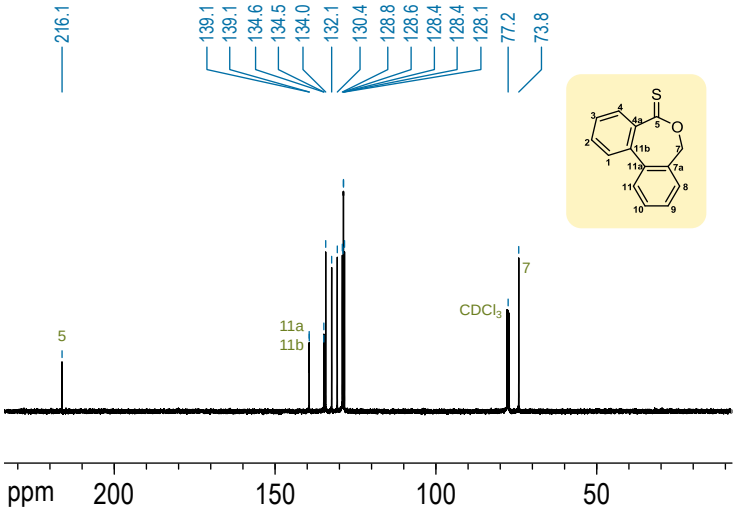

Figure S2. Full ^{13}C NMR spectrum (101 MHz, $CDCl_3$) of dibenzo[c,e]oxepan-5-thione.

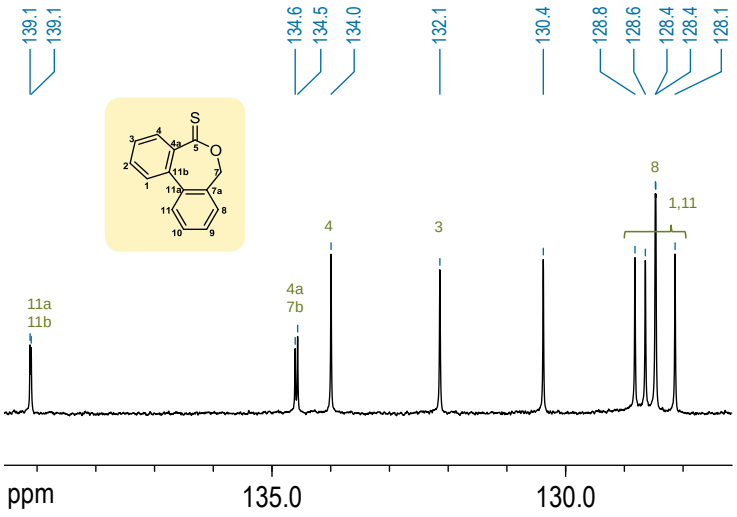

Figure S3. Section of ^{13}C NMR spectrum (101 MHz, $CDCl_3$) of dibenzo[c,e]oxepan-5-thione expanding the aromatic region.

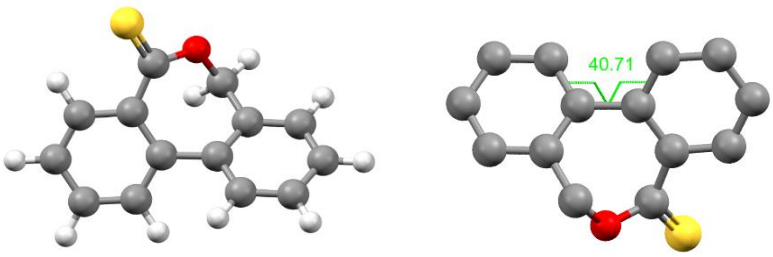

Figure S4. DFT-optimised structure of dibenzo[c,e]oxepan-5-thione with the dihedral angle indicated in the right image.

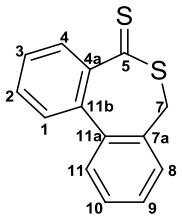

(side product)
$C_{14}H_{10}S_2$
242.35 gmol^{-1}

The above reaction also afforded a red solid (0.12 g, 2%), identified as dibenzo[c,e]thiepane-5-thione.

^{1}H NMR (400 MHz, $CDCl_3$) δ/ppm = 7.87 (dd, *J* = 7.9, 1.2 Hz, 1 H), 7.55 (td, *J* = 7.6, 1.4 Hz, 1 H), 7.46–7.30 (m, 5 H), 7.26 (d, *J* = 8.4 Hz, 1 H), 4.40 (d, *J* = 13.8 Hz, 1 H), 3.51 (d, *J* = 13.8 Hz, 1 H).

^{13}C NMR (101 MHz, $CDCl_3$) δ/ppm = 234.07 (**5**), 145.92, 138.64, 135.81, 131.51, 130.62, 130.25, 129.80, 128.79, 128.64, 128.08, 126.36, 39.69 (**7**).

IR ν_{max}/cm^{-1} = 3057 (w, CH), 3024 (w, CH), 2920 (w, CH), 2850 (w, CH), 1627 (m, C=C), 1593 (m, C=C), 1554 (m, C=C), 1196 (m, C=S).

Rf 0.81 (EtOAc–Pet. Ether, 1:2)

3.7) Dibenzo[c,e]thiepan-5-one

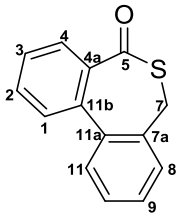

$C_{14}H_{10}OS$
226.29 gmol^{-1}

Dibenzo[c,e]oxepan-5-thione (DOT) (16.3 mg) was dissolved in DMSO-d_6 (600 µL) and heated overnight to 150 °C.

^{1}H NMR (400 MHz, DMSO-d_6) δ/ppm = 7.73 (td, *J* = 7.8 Hz, 1.72, 1 H), 7.63-7.57 (m, 2 H), 7.49–7.41 (m, 5 H), 4.15 (d, *J* = 14.1 Hz, 1 H, **7**), 3.98 (d, *J* = 14.1 Hz, 1 H, **7**).

^{13}C NMR (101 MHz, DMSO-d_6) δ/ppm = 198.6 (**5**), 139.5, 137.6, 137.4, 137.0, 132.6, 130.6, 130.5, 128.8, 128.5, 128.5, 128.1, 126.8, 34.0 (**7**).

4) Determination of reactivity ratios, r_{DOT} and r_{MA}

4.1) Data Acquisition

The copolymerization behaviour between DOT and methyl acrylate (MA), as a model acrylic monomer, was determined through AIBN-initiated free-radical polymerization in deuterated acetonitrile as solvent. DOT (**6**) and methyl acrylate (in varying molar ratios, 100 eq total), acetonitrile-d_3 (1–2 mL) and AIBN (1 eq) were mixed and degassed by bubbling nitrogen for 20 min. The mixtures were heated to 80 °C until overall low monomer conversions were reached (several hours needed for DOT-rich formulations due to retardation). After cooling to RT, the mixtures were analysed by ^{1}H NMR spectroscopy.

^{1}H NMR (400 MHz, $CDCl_3$) δ/ppm = 8.10 (d, 1 H of residual DOT monomer), 7.18 (bm, 4 H of DOT in polymer), 6.34, 6.16, 5.84 (3 × dd, 1 H each of res. MA monomer), 5.29, 5.16 (2 × d, 1 H each of res. DOT monomer), 3.99 (m, backbone C*H*–SCO), 3.74–3.50 (m, OCH_3 of MA in monomer and polymer).

From the NMR integrals, the following values were determined (see Table S1):

- average **mole fraction** of DOT in the monomer feed during the polymerization, f_{DOT}
- **mole fraction** of DOT in the copolymers, F_{DOT}
- average **concentration ratio**, x_{DOT} =[DOT]/[MA], of DOT in the monomer feed during the polymerization
- **concentration ratio** of DOT in the copolymers, X_{DOT}

Table S1. Overview of measured and calculated data of DOT–MA copolymer samples with varying comonomer feed compositions

	A	B	C	D	E	F	G	H	I	J	K	L	M	N	O
Sample	**Time (h)**	**Res. DOT Mono. (1 H)** 8.1 ppm [g]	**DOT in Polym. (4 H)** 7.2 ppm	**Total DOT (1 H)** =B+(C/4) [h]	**Res. MA Mono. (1 H)** 6.3, 6.2, 5.8 ppm (ave.)	**Total MA (3 H)** 3.7 ppm	**MA in Polym. (1 H).** =(F/3)−E	**DOT conv. (%)** =100× (C/4)/D	**MA conv. (%)** =100× G	f_{DOT}^{0} [a] =D/(D+(F/3))	f_{DOT}^{end} [b] =B/(B+E)	f_{DOT} [c] =0.5(J+K)	F_{DOT} [d] =(C/4)/((C/4)+G)	x_{DOT} [e] =L/(1−L)	X_{DOT} [f] =M/(1−M)
①	0.8	0.07	0.08	0.0900	0.8333	3.00	0.1667	22	17	0.0826	0.0775	0.0800	0.1071	0.0870	0.1200
②	1.5	0.11	0.18	0.1550	0.8067	3.00	0.1933	29	19	0.1342	0.1200	0.1271	0.1888	0.1456	0.2328
③	1.1	0.28	0.17	0.3225	0.8933	3.00	0.1067	13	11	0.2439	0.2386	0.2412	0.2849	0.3180	0.3983
④	1.0	0.33	0.32	0.4100	0.8600	3.00	0.1400	20	14	0.2908	0.2773	0.2840	0.3636	0.3967	0.5714
⑤	2.0	0.39	0.39	0.4875	0.8500	3.00	0.1500	20	15	0.3277	0.3145	0.3211	0.3939	0.4730	0.6500
⑥	1.1	0.52	0.12	0.5500	0.9467	3.00	0.0533	5	5	0.3548	0.3545	0.3547	0.3601	0.5496	0.5629
⑦	1.4	0.47	0.20	0.5200	0.9067	3.00	0.0933	10	9	0.3421	0.3414	0.3418	0.3489	0.5192	0.5359
⑧	5.0	0.84	0.48	0.9600	0.8233	3.00	0.1767	13	18	0.4898	0.5050	0.4974	0.4044	0.9897	0.6791
⑨	6.0	1.26	0.78	1.4550	0.7900	3.00	0.2100	13	21	0.5927	0.6146	0.6037	0.4815	1.5230	0.9286
⑩	5.5	1.71	0.24	1.7700	0.9067	3.00	0.0933	3	9	0.6390	0.6535	0.6462	0.3914	1.8268	0.6431
⑪	6.0	2.28	0.59	2.4275	0.8233	3.00	0.1767	6	18	0.7082	0.7347	0.7215	0.4550	2.5903	0.8347
⑫	6.0	3.49	0.45	3.6025	0.8833	3.00	0.1167	3	12	0.7827	0.7980	0.7904	0.4908	3.7704	0.9640
⑬	6.0	8.86	1.35	9.1975	0.6600	3.00	0.3400	4	34	0.9019	0.9307	0.9163	0.4982	10.9481	0.9926

[a] Initial mole fraction of DOT in the monomer feed

[b] Mole fraction of DOT in the residual monomer mixture

[c] The average of the initial and final mole fraction of DOT was used to express conditions during the copolymerization. Even at higher conversions above 20%, the differences between initial and final concentration of monomers were not large (compare columns J and K).

[d] Mole fraction of DOT in the copolymer

[e] Concentration *ratio* of DOT in the monomer feed

[f] Concentration *ratio* of DOT in the copolymer

[g] Measured value of ^{1}H NMR integral as indicated. The integration was normalized to the signal of all methoxy groups (= 3.00 H)

[h] Calculated value. Bold letters refer to column.

4.2) Non-linear regression; mole fractions

The most statistically sound method to determine reactivity ratios is to fit a plot of the instantaneous copolymer composition versus the comonomer feed composition.[3]

The copolymer **mole fraction** F_{DOT} was plotted against the feed **mole fraction**, f_{DOT}.
(columns **L** and **M** from above table)
The data was fitted using the Mayo-Lewis equation in its mole fraction form,[3]

$$F_{DOT}^{calc} = \frac{r_{DOT} f_{DOT}^2 + f_{DOT}(1 - f_{DOT})}{r_{DOT} f_{DOT}^2 + 2 f_{DOT}(1 - f_{DOT}) + r_{MA}(1 - f_{DOT})^2}$$

where r_{DOT} and r_{MA} are the reactivity ratios for DOT and MA, respectively.

The data was fitted using Microsoft Excel so that the sum of squares, $\sum\left(F_{DOT} - F_{DOT}^{calc}\right)^2$ was minimal. This was achieved for $r_{DOT} = 0.0030$ and $r_{MA} = 0.424$. The average deviation of the fitted curve from each measured data point was $\sqrt{\frac{\sum\left(F_{DOT} - F_{DOT}^{calc}\right)^2}{n}} = 0.029$, where *n* is the number of samples.

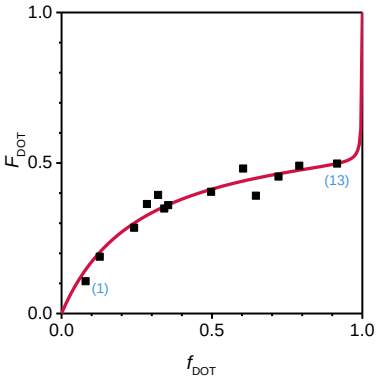

Figure S5. Non-linear fitting based on mole fractions (as shown in main text). For easier interpretation, numbers of samples ① and ⑬ are added. This method has the advantage that non-manipulated data is fitted, that all data points are equally weighed, that it is straightforward to select suitable comonomer feed compositions (e.g. in steps of f = 0.1), and that it produces an easy-to-interpret plot of meaningful quantities. Note that the mole fraction plots, unlike those in Figures 7–13, allow to depict the positions of both homopolymers at f_{DOT}, F_{DOT} = 0, 0 and 1, 1, respectively. Result: $r_{DOT} = 0.0030,\ r_{MA} = 0.424$

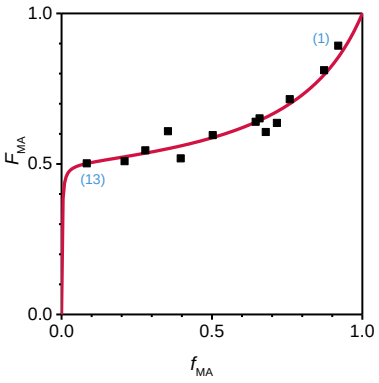

Figure S6. Another advantage of fitting based on mole fractions is that the method is insensitive to an inversion of the monomer roles, *i.e.* plotting $F_{MA} = 1 - F_{DOT}$ against $f_{MA} = 1 - f_{DOT}$. The same results are obtained with the same average deviation of data points from the curve.
Result: $r_{DOT} = 0.0030,\ r_{MA} = 0.424$

4.3) Non-linear regression; concentration ratios

The Mayo-Lewis equation is more commonly quoted in its (easier derivable) concentration ratio form,[3]

$$X_{DOT}^{calc} = x_{DOT}\frac{x_{DOT}r_{DOT} + 1}{r_{MA} + x_{DOT}}$$

where $x_{DOT} = \frac{[DOT\ in\ monomer\ feed]}{[MA\ in\ monomer\ feed]}$ and $X_{DOT} = \frac{[DOT\ in\ copolymer]}{[MA\ in\ copolymer]}$, with the reactivity ratios as defined above.

For comparison, this method was also used for curve fitting (columns **N** and **O** from above table)

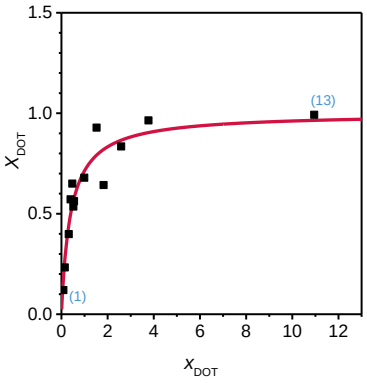

Figure S7. Non-linear fitting based on concentration ratios. In this method, data points with higher X_{DOT} gain more influence because their absolute values are higher (a DOT homopolymer would be represented in this plot as $X_{DOT} \to \infty$). The plot is therefore sensitive to an inversion of the monomer assignments. Result: $r_{DOT} = 0.0026,\ r_{MA} = 0.405$

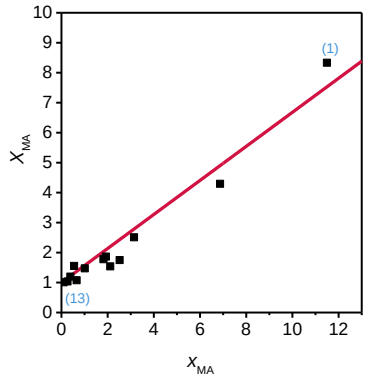

Figure S8. For comparison: non-linear fitting based on concentration ratios with exchanged roles of monomers. Plotted here are $X_{MA} = (X_{DOT})^{-1}$ against $x_{MA} = (x_{DOT})^{-1}$. Note that this plot is overinflated for DOT-poor formulations (lower sample numbers), which dominate the curve fitting. Result: $r_{DOT} = 0.034,\ r_{MA} = 0.573$

4.4) Linear Fitting: Fineman–Ross

Concept: $G = r_1 H - r_2$; here: $r_1 = r_{DOT}$ and $r_2 = r_{MA}$

with $G = \frac{x\,(X-1)}{X}$ and $H = \frac{x^2}{X}$, where x and X are the concentration ratios [DOT]/[MA] in the feed mixture and the copolymer respectively (columns **N** and **O** in above table)

The reactivity ratios are then obtained as $r_1 = \text{slope}$ and $r_2 = -\text{intercept}$.

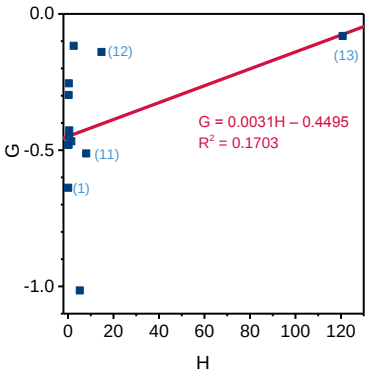

Figure S9. Fineman–Ross plot of the above data. The plot is dominated by sample ⑬ and has a poor correlation coefficient.

Result: $r_{DOT} = 0.0031,\ r_{MA} = 0.4495$

If the right-most data point is removed, the result is $r_{DOT} = 0.0077,\ r_{MA} = 0.4617$, indicating that the fit does not rely solely on this data point (as the graph might suggest).

4.5) Linear Fitting: Inverted Fineman–Ross

Using the inverted Fineman–Ross plot has the same effect as changing the roles of the two comonomers in the regular Fineman–Ross plot and vice versa.

Concept: $\frac{G}{H} = -r_2 \frac{1}{H} + r_1$; here: $r_1 = r_{DOT}$ and $r_2 = r_{MA}$ with definitions as above.

The reactivity ratios are then obtained as $r_1 = \text{intercept}$ and $r_2 = -\text{slope}$.

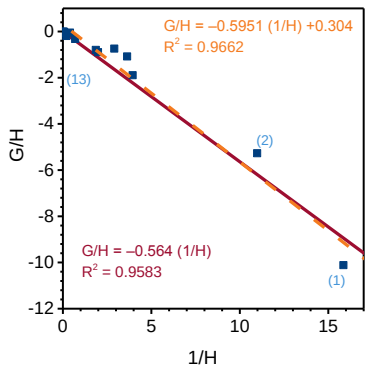

Figure S10. Inverted Fineman–Ross plot. The data points are more evenly spread out. The fit gives: $r_{DOT} = 0.304,\ r_{MA} = 0.5951$ with a good correlation ($R^2 = 0.9662$, orange dashed line). If the fit is forced through an intercept of zero, $r_{DOT} = 0$ (set), $r_{MA} = 0.564$ with a good correlation ($R^2 = 0.9583$, red solid line).

4.6) Linear Fitting: Yezrielev–Brokhina–Roskin

Concept: $G = r_1 H^{1.5} - r_2$; here: $r_1 = r_{DOT}$ and $r_2 = r_{MA}$ with definitions as above.

The reactivity ratios are then obtained as $r_1 =$ slope and $r_2 = -$intercept.

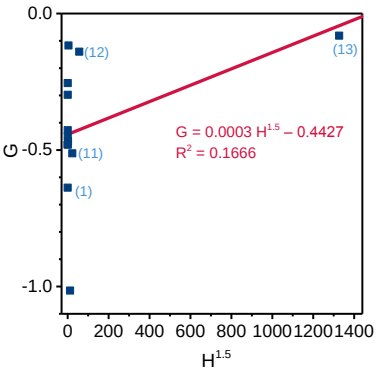

Figure S11. Yezrielev–Brokhina–Roskin plot. The plot is even more grossly inflated toward sample ⑬ than the F–R plot and has a poor correlation.

Result: $r_{DOT} = 0.0003,\ r_{MA} = 0.4427$

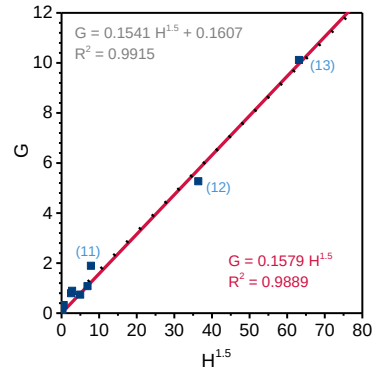

Figure S12. For comparison: YBR plot with inverted monomer roles, i.e. $r_1 = r_{MA}$ and $r_2 = r_{DOT}$. The plot was constructed by using the inverse values from columns **N** and **O** in the above table, according to $X_{MA} = (X_{DOT})^{-1}$ and $x_{MA} = (x_{DOT})^{-1}$. Result: $r_{DOT} = -0.1607,\ r_{MA} = 0.1541$. The negative value for r_{DOT} does not make sense (black dotted line). If the fit is forced through an intercept of $G = 0$, $r_{DOT} = 0$ (set), $r_{MA} = 0.1579$ (red solid line).

4.7) Linear Fitting: Kelen–Tüdős

Concept: $\eta = \left(r_1 + \frac{r_2}{\alpha}\right)\xi - \frac{r_2}{\alpha}$; here: $r_1 = r_{DOT}$ and $r_2 = r_{MA}$ with

$\alpha = \sqrt{H_{min} H_{max}} = 2.7595,\ \ \eta = \frac{G}{\alpha + H},\ \ \xi = \frac{H}{\alpha + H}$, with G and H defined as above.

The reactivity ratios are then obtained as $r_1 =$ slope + intercept and $r_2 = -$intercept × α.

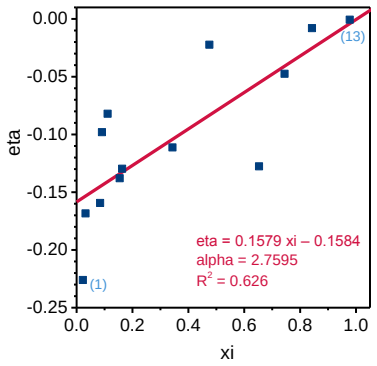

Figure S13. KT plot of above data.

Result: $r_{DOT} = -0.00056,\ r_{MA} = 0.4372$. The negative value for r_{DOT} does not make sense and should be interpreted as $r_{DOT} \approx 0$. An exchange of the monomer roles, i.e. $r_1 = r_{MA}$ and $r_2 = r_{DOT}$ based on recalculated values of G and H using $X_{MA} = (X_{DOT})^{-1}$ and $x_{MA} = (x_{DOT})^{-1}$ leads to the same result (plot not shown).

4.8) Summary of Methods to Determine Reactivity Ratios

Table S2. Overview of reactivity ratios determined for DOT–MA

Method	**Assignment of r_1 and r_2**	r_{DOT}	r_{MA}	**Measure of Goodness with value**	**Authors' comments based on current data set**
Non-linear least-square fitting of mole fractions	*irrelevant*	0.0030	0.424	Average deviation of fitted curve from data points, $\sqrt{\frac{\sum(F_{DOT}-F_{DOT}^{calc})^2}{n}} = 0.029$	most reliable method
Non-linear least-square fitting of concentration ratios	$r_1 = r_{DOT}$; $r_2 = r_{MA}$	0.0026	0.405	Average deviation of fitted curve from data points, $\sqrt{\frac{\sum(X_{DOT}-X_{DOT}^{calc})^2}{n}} = 0.078$	unequal weighting of data points
Non-linear least-square fitting of concentration ratios	$r_1 = r_{MA}$; $r_2 = r_{DOT}$	0.034	0.573	Average deviation of fitted curve from data points, $\sqrt{\frac{\sum(X_{DOT}-X_{DOT}^{calc})^2}{n}} = 0.41$	unequal weighting; dominated by few data points
Linear fitting: Fineman–Ross	$r_1 = r_{DOT}$; $r_2 = r_{MA}$	0.0031	0.4495	Correlation coefficient, $R^2 = 0.1703$	unequal weighting; dominated by few data points; poor correlation
Linear fitting: inverted Fineman–Ross	$r_1 = r_{DOT}$; $r_2 = r_{MA}$	0.304	0.5951	Correlation coefficient, $R^2 = 0.9662$	reasonably good fit; unequal weighting; disagreement with other methods in value of r_{DOT}
Linear fitting: inverted Fineman–Ross	$r_1 = r_{DOT}$; $r_2 = r_{MA}$	0 (set)	0.564	Correlation coefficient, $R^2 = 0.9583$	reasonably good fit; unequal weighting; required deliberate adjustment of r_{DOT}
Linear Fitting: Yezrielev–Brokhina–Roskin	$r_1 = r_{DOT}$; $r_2 = r_{MA}$	0.0003	0.4427	Correlation coefficient, $R^2 = 0.1666$	unequal weighting; dominated by few data points; poor correlation
Linear Fitting: Yezrielev–Brokhina–Roskin	$r_1 = r_{MA}$; $r_2 = r_{DOT}$	0 (set)	0.1579	Correlation coefficient, $R^2 = 0.9889$	reasonably good fit; unequal weighting; result does not agree with other methods (including YBR fit with exchanged monomer roles); required deliberate adjustment of r_{DOT}
Linear Fitting: Kelen–Tüdős	*irrelevant*	≈ 0	0.4372	Correlation coefficient, $R^2 = 0.626$	data points evenly spaced; lower correlation coefficient

5) Free radical copolymerizations of DOT

5.1) Free radical copolymerization of DOT and methyl acrylate

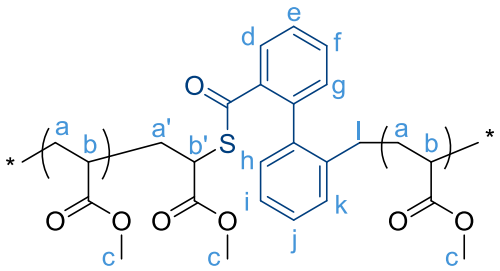

DOT (**6**, 95 mg, 0.419 mmol, 23 eq.), methyl acrylate (127 µL, 1.403 mmol, 77 eq.), anisole (1.5 mL) and AIBN (3 mg, 0.018 mmol, 1 eq.) were mixed together, sealed with a septum and degassed by bubbling nitrogen for 30 min. The mixture was then heated to 80 °C for 19.5 hours before being cooled to RT and exposed to air. The polymer was purified by precipitation into diethyl ether (approximately 30-fold in volume) and the polymer was collected as a white solid by centrifugation followed by drying in a vacuum at room temperature. Conversions 84% (DOT), 81% (MA); poly(DOT_{19}-*co*-MA_{62}); M_n^{theor} = 9.7 kg/mol.

^{1}H NMR (400 MHz, $CDCl_3$) δ/ppm = 7.74 (d), 7.54 + 7.44 (e, f), 7.19 (g, h, i, k), 7.04 (j), 4.11 (b'), 3.66 (c), 2.31 (b, l), 1.93 + 1.68 + 1.52 (a, a')

SEC. M_n^{SEC} = 10.3 kg/mol, $Đ$ = 1.79.

5.2) Free radical copolymerization of DOT and acrylonitrile

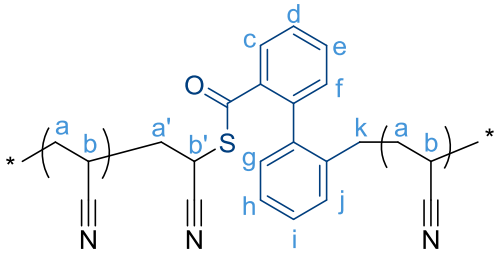

DOT (**6**, 20.3 mg, 0.090 mmol, 3.7 eq), acrylonitrile (99 µL, 2.303 mmol, 96.3 eq.), anisole (1.0 mL) and AIBN (4.0 mg, 0.024 mmol, 1 eq.) were mixed together, sealed with a septum and degassed by bubbling nitrogen for 30 min. The mixture was heated to 80 °C for 16.5 h before being cooled to RT and exposed to air. The mixture was purified by precipitation into diethyl ether (40 mL) and the polymer was collected as a white solid by centrifugation followed by drying in a vacuum at room temperature.

^{1}H NMR (400 MHz, DMSO-d_6) δ/ppm = 7.89 (c), 7.71 + 7.62 (d, e), 7.36 (f, g, h, j), 7.08 (i), 4.56 (b'), 3.12 (b), 2.03 (a, a', k)

SEC. *polymer insoluble in THF*

5.3) Free radical copolymerization of DOT and N,N-*dimethyl acrylamide (DMAA)*

DOT (**6**, 50.6 mg, 0.224 mmol, 4.9 eq.), DMAA (456 µL, 4.419 mmol, 96.1 eq.), anisole (1.5 mL) and AIBN (7.6 mg, 0.046 mmol, 1 eq.) were mixed together, sealed with a septum and degassed by bubbling nitrogen for 30 min. The mixture was heated to 80 °C for 19.5 h before being cooled to RT and exposed to air. The mixture was purified by precipitation into diethyl ether (40 mL) and the polymer was collected as a white solid by centrifugation followed by drying in a vacuum at room temperature. Conversions: 100% (DOT), 100% (DMAA); poly(DOT_5-*co*-$DMAA_{96}$); M_n^{theor} = 10.6 kg/mol.

^{1}H NMR (400 MHz, $CDCl_3$) δ/ppm = 7.66 (e), 7.51 + 7.41 (f, g), 7.21 (h, i, j, l), 7.00 (k), 4.38, 4.21 (b'), 3.10–2.50 (c), 2.62 (b,c,m), 1.80–1.10 (a, a')

SEC. M_n^{SEC} = 6.7 kg/mol, $Đ$ = 1.73.

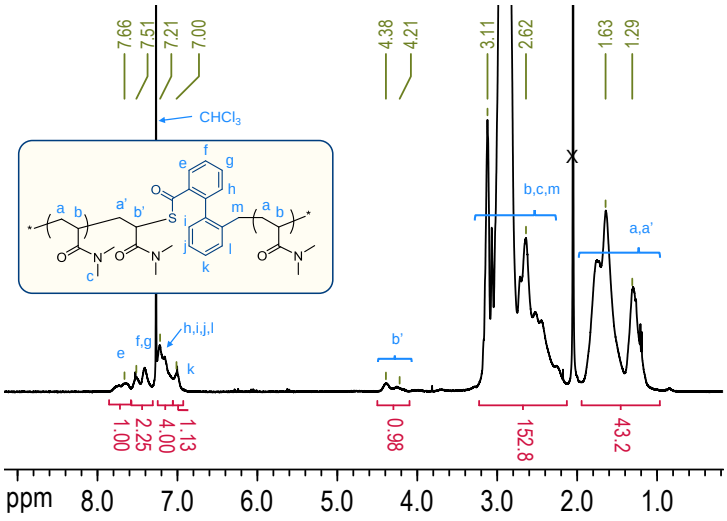

Figure S14. ^{1}H NMR spectrum (400 MHz, $CDCl_3$) of poly(DOT_5-co-$DMAA_{96}$) with assignments. The splitting of signal b' is presumed to stem from backbone tacticity.

6) RAFT copolymerization of PEGA and DOT

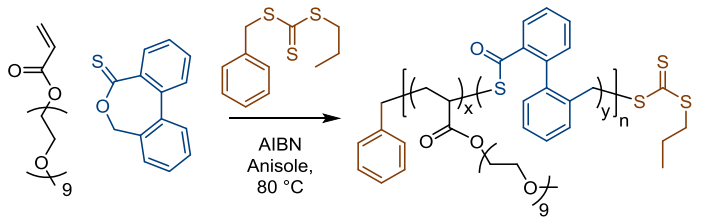

DOT and PEGA (see table for ratio), *S*-benzyl-*S*-propyl trithiocarbonate[4] (1 eq.), AIBN (0.25 eq.) and anisole (total monomer conc. =1.55 M) were added into a ground-glass joint tube. The reaction was sealed with a rubber septum, stirred and degassed with nitrogen for 30 min through a needle, with a shorter needle fitted for gas release. The tube was then placed in a pre-heated oil bath set at 80 °C and left overnight (16.5 hours). After cooling and exposing to air, the monomer conversion was determined by ^{1}H NMR analysis. The crude polymer solution was purified by dialysis against methanol in regenerated cellulose membranes (3500 gmol^{-1} molecular weight cut-off) and the polymers were isolated by freeze-drying as viscous yellow liquids.

^{1}H NMR (400 MHz, $CDCl_3$) δ/ppm = 7.71 (e), 7.42 (f, g), 7.23 (h, i, j, l), 6.98 (k), 4.15 (c), 4.06 (b'), 3.63 (PEG), 3.37 (d), 2.28 (b, m), 1.87 + 1.60 (a, a') (see main text for assignments)

^{13}C NMR (101 MHz, $CDCl_3$) δ/ppm = 192.6 + 191.1 (SC=O), 174.2 + 170.8 (OC=O), 139.5 (quat. C_{Ar}), 131.5 (C_{Ar}-H), 129.6 (k), 128.0 (e), 125.7 (C_{Ar}-H), 71.9 (PEG), 70.6 (PEG), 68.8 (PEG), 64.4 + 63.3 (c), 59.0 (d), 46.2 + 43.9 + 42.8 + 41.1 (b, b'), 34.0 + 31.8 (a), 30.6 (m).

IR ν_{max}/cm^{-1} = 2870 (m, CH), 1732 (m, OC=O, PEGA), 1678 (w, SC=O, DOT), 907 (m, C-S, DOT)

Table S3. Overview of RAFT polymerizations.[a]

Code	Feed		f_{DOT}[b]	Conversion[c]		Composition[c]	M_n[c]	F_{DOT}^{conv}[d]	F_{DOT}^{NMR}[e]	M_n^{SEC}[f]	$Đ^{SEC}$[f]
	DOT (eq)	PEGA (eq)		DOT (%)	PEGA (%)	DOT (DP) + PEGA (DP)	(kg/mol)				
polyPEGA	0	250	0	–	99	0 + 248	119	0	0	13.5	1.36
poly(DOT_2-*co*-$PEGA_{244}$)	2	248	0.008	100	98	2 + 244	117	0.01	0.01	17.4	1.23
poly(DOT_5-*co*-$PEGA_{235}$)	5	245	0.02	100	96	5 + 235	114	0.02	0.03	19.0	1.32
poly(DOT_{11}-*co*-$PEGA_{230}$)	12.5	237.5	0.05	85	97	11 + 230	113	0.05	0.07	13.2	1.36
poly(DOT_{26}-*co*-$PEGA_{141}$)	30	220	0.12	87	64	26 + 141	74	0.16	0.17	25.5	1.19
poly(DOT_{20}-*co*-$PEGA_{46}$)	50	200	0.2	39	23	20 + 46	27	0.30	0.36	15.2	1.25
poly(DOT_{22}-*co*-$PEGA_{64}$)[g]	40	160	0.2	55	40	22 + 64	36	0.26	0.24	11.6	1.22

[a] Polymerizations followed the above general procedure, unless noted otherwise
[b] Mole fraction of DOT in monomer mixture
[c] Determined from ^{1}H NMR spectrum of crude polymerization mixture
[d] Mole fraction of DOT in copolymer based on conversions
[e] Mole fraction of DOT in copolymer based on ^{1}H NMR spectrum of purified copolymers
[f] Determined by size exclusion chromatography
[g] Polymer prepared using 0.2 eq of AIBN and polymerised for 18.5 hours instead of 16.5 hours

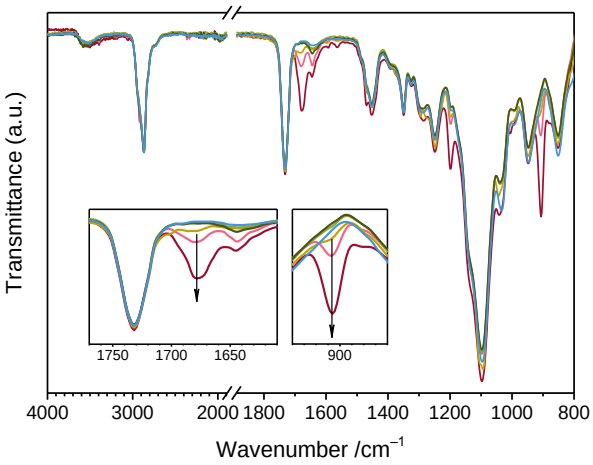

Figure S15. FT-IR spectra of polyPEGA (light blue curve) and poly(DOT-*co*-PEGA) copolymers (details in Table S3). The insets show the bands assigned to the thioester SC=O stretching vibration (ν = 1678 cm^{-1}) and C–S stretching vibration (ν = 907 cm^{-1}) that increased with the DOT feed ratio.

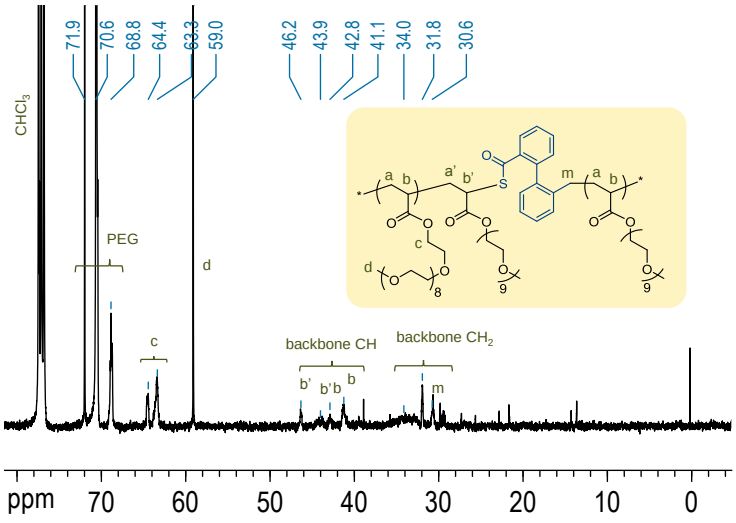

Figure S16. Section of ^{13}C NMR spectrum (101 MHz, $CDCl_3$) of poly(DOT_{20}-*co*-$PEGA_{46}$) with assignment.

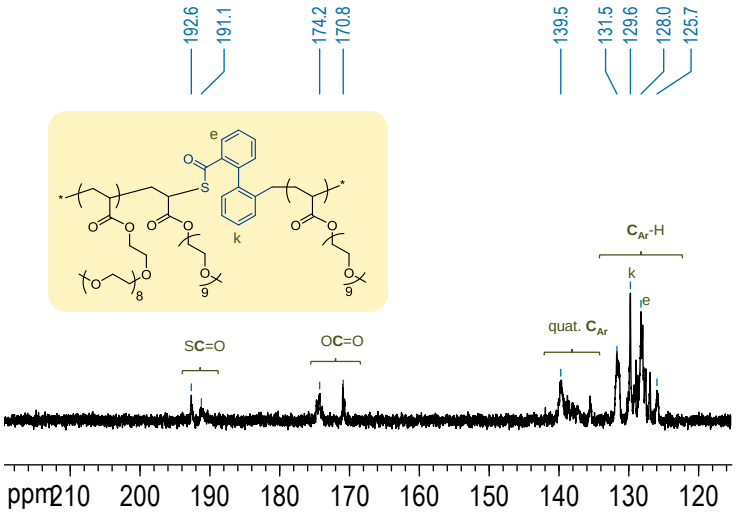

Figure S17. Section of ^{13}C NMR spectrum (101 MHz, $CDCl_3$) of poly(DOT_{20}-*co*-$PEGA_{46}$) with assignment. The splitting of the carbonyl signals is presumed to stem from backbone tacticity.

7) Degradation Experiments

7.1) Isopropylamine

Poly(DOT_x-*co*-$PEGA_y$) or polyPEGA (2 mg) was dissolved in dichloromethane (1 mL) before isopropyl amine (1 mL) was added. This large amount of amine was chosen to ensure complete degradation. The mixture was stirred in a sealed vial overnight. Solvent and amine were evaporated by blowing in nitrogen gas and the residue was dissolved in THF and analysed by SEC.

7.1) Methanol control

Poly(DOT_x-*co*-$PEGA_y$) (2 mg) was dissolved in methanol (2 mL), stirred overnight and analysed as above.

8) References

1. X. Sheng, K. Hua, C. Yang, X. Wang, H. Ji, J. Xu, Z. Huang and Y. Zhang, *Bioorganic & Medicinal Chemistry Letters*, 2015, **25**, 3535-3540.
2. V. Brandmeier and M. Feigel, *Tetrahedron*, 1989, **45**, 1365-1376.
3. G. Odian, *Principles of Polymerization*, John Wiley & Sons, Inc., 4. edn., 2004.
4. J. Y. Quek, P. J. Roth, R. A. Evans, T. P. Davis and A. B. Lowe, *Journal of Polymer Science Part A: Polymer Chemistry*, 2013, **51**, 394-404.